Equal Thermodynamic Distance and Equipartition of Forces Principles Applied to Binary Distillation†

Erik Sauar,‡ Gino Siragusa,§ and Bjarne Andresen*,||

Department of Physical Chemistry, NTNU, N-7034 Trondheim, Norway, Department of Chemistry, San Diego State University, San Diego, California 92182, Ørsted Laboratory, University of Copenhagen, Universitetsparken 5, DK-2100 Copenhagen Ø, Denmark

Received: September 28, 2000; In Final Form: December 13, 2000

Two theoretically derived entropy optimization methods for design of distillation columns with multiple heat exchangers have recently been presented in the literature. These two methods, called equal thermodynamic distance (ETD) and equipartition of forces (EoF), have here been applied to binary distillation and compared. For a 17 plate column separating benzene and toluene the entropy production inside the ETD column was found to be 32.8% less than the comparable adiabatic column while the entropy production in the EoF column was 32.6% less. A numerically calculated optimum was found to be 37.3% better than the adiabatic column. The difference between the EoF column and the numerical optimum occurs mainly in the end sections where the EoF operating line requires driving forces which are difficult to obtain because of the mass balance. The mismatch is mainly due to (i) failure to take bulk fluxes into account, (ii) mass balance restrictions on the driving force in the upper section, and (iii) uncertainty in the application of the Gibbs−Duhem equation. The ETD column differs from the numerical optimum much in the same manner as the EoF column, by requiring step sizes in the end sections which mass balance only allows at high entropy costs. For very large plate numbers, however, the ETD column is almost in complete agreement with the numerical optimum.

1. Introduction

Distillation is a multistage separation process of a liquid or vapor mixture of two or more components. While an adiabatic distillation column only exchanges heat in the reboiler and the condenser, normally located at the bottom and at the top of the column, the columns studied here have heat exchangers integrated on the plates inside the column, as is shown in Figure 1. *Reversible* distillation (with continuous heat exchange) has been described by for instance King,[13] Fonyo,[11] and Kaiser and Gourlia.[12] Such columns are of infinite length and are mainly of theoretical interest, used for modeling purposes or used to find lower bounds on the energy input. A more practical approach has been taken by Terranova and Westerberg,[30] Agrawal and Fidkowski,[2] Aguirre et al.,[1] and Kjelstrup Ratkje et al.,[19] who have studied the effects of and conditions for applying *one or more intermediate heat exchangers*, without adding more than a limited number of additional plates. The current work represents a compromise between these two approaches by asking how heat should be added to or withdrawn from each plate while the total number of plates is given. It is thus a quest for the most *near-reversible real column* rather than for the ideal reversible column itself.

The motivation for distillation columns with distributed heat supply and removal is the reduction of exergy losses or entropy production which can be obtained, because an increase in the entropy production of a system reduces the available work.

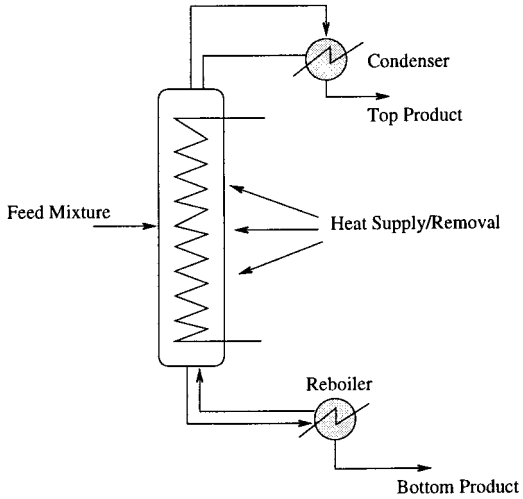

Figure 1. Distillation columns considered have local heat exchangers on all plates.

Tolman and Fine's equality[31] highlights this relation:

$$\dot{W}_R = \Delta\dot{E}x - T_0\Delta\dot{S}^{irr} \quad (1)$$

Here $\dot{W}_R$ is the power extracted from a nonequilibrium process, $\Delta\dot{E}x$ is the exergy change per unit time, $\Delta\dot{S}^{irr}$ is the irreversible entropy production rate, and T_0 is the environment temperature. For distillation processes, W_R is the reversible separation work, ΔG_{unmix} delivered, and ΔEx is the exergy provided through the heat flows. The equation shows that minimization of entropy production is equivalent to minimizing exergy lost due to the way the process is set up, or equivalently to maximizing separation work for a given exergy supply ΔEx.

† Part of the special issue "Aron Kuppermann Festschrift".

* To whom correspondence should be addressed.
‡ NTNU. E-mail: sauar@chembio.ntnu.no.
§ San Diego State University. E-mail: gino@math.sdsu.edu.
|| University of Copenhagen. E-mail: andresen@fys.ku.dk. Fax: +45-35320460.

10.1021/jp003555p CCC: $20.00
Published on Web 02/20/2001

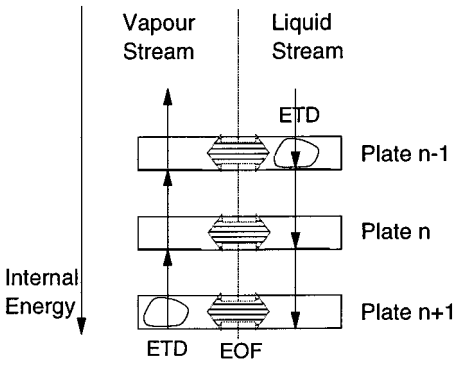

Figure 2. Equal thermodynamic distance (ETD) vs equipartition of forces (EoF) principles. ETD optimizes the movement of an open system exchanging mass and heat with its surroundings at discrete equilibrium points in state space. EoF optimizes the exchange of mass and heat between the vapor and liquid streams.

Two theoretically derived energy optimization methods for design of distillation columns with distributed heat exchange have recently been presented in the literature. The design principle called equal thermodynamic distance (ETD) has been derived from finite-time thermodynamics[4,5,20] and states that a system which is allowed to exchange heat and mass with its surroundings at a given number of discrete points of equilibrium (here the plates) should go from one thermodynamic state to another in equally long steps according to the Weinhold metric[32] in thermodynamic state space in order to minimize the total entropy production.[14] This general result has later been made explicit for binary distillation,[6,21] recommending that the thermodynamic distance between each pair of plates should be made equal. The Weinhold metric and thermodynamic distance will be described further in section 2.

The equipartition of forces (EoF) design principle[28] says that two process streams exchanging heat or matter should do so with a uniform driving force over the surface area (transfer area) between them in order to minimize exergy losses. In binary distillation the vapor and liquid streams are such two process streams exchanging heat and matter, and the gas−liquid interphase is the transfer area between them. The theoretical principle was obtained from irreversible thermodynamics combined with the Onsager relations and Lagrange optimization procedures. Operating lines designed with uniform driving forces will here be referred to as "EoF operating lines".

Using a numerical algorithm, Rivero[16,17] found that the minimum exergy loss in diabatic (e.g. distributed heat exchange) binary distillation is obtained with an operating "line" being largely parallel to the equilibrium curve in a McCabe−Thiele diagram. This result resembles the EoF method,[28] and a joint study was conducted following Sauar et al.[24] showing that there was a high degree of consistency between the numerically optimal column and the EoF column in the sections where large reflux ratios were avoided.[24] The reliability of the result, however, suffered from the fact that the numerically optimal column in Rivero's original study did not perform the same separation work as the adiabatic column it was compared with.

As illustrated in Figure 2, the two theoretical principles have quite different starting points. The EoF lines are the result of an optimization considering the countercurrent exchange of components between the liquid and the vapor streams. The ETD path has been derived considering the stepwise movement of an open system (the "amoeba" in the figure) from one end of the column reaching thermal and chemical (i.e. compositional) equilibrium on each of the plates.

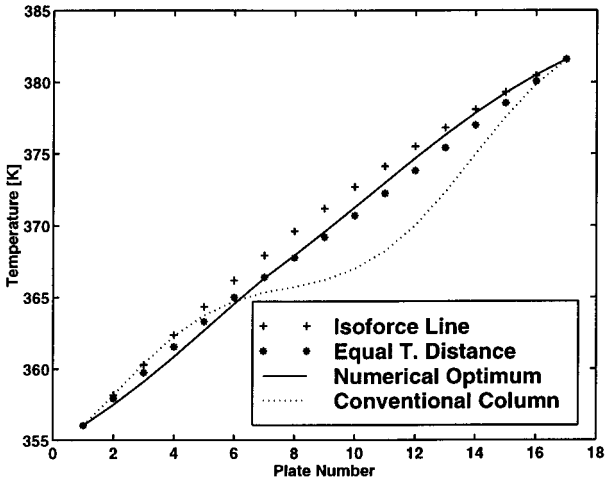

Figure 3. Temperature profiles as functions of plate number for the EoF, the ETD, the conventional adiabatic, and the numerically optimized column.

In this paper we present simulations of binary distillation columns designed according to these two theoretical principles and compare their performance. We also compare them with a numerically optimized design and discuss the deviations between the theoretically derived optima and the numerical one.

2. Design by Equal Thermodynamic Distance

The internal distribution of temperature and mole fractions in a conventional distillation column, where heat is added and withdrawn only in the reboiler and the condenser, respectively, is fixed exclusively by the laws of energy and mass conservation. In many conventional columns that leads to an S-shaped curve of temperature versus plate number with most of the variation occurring near the end points of the column, connected with a flat stretch (pinch) around the feed point (see Figure 3). A qualitatively similar picture emerges for the mole fractions. If the number of plates is increased in a conventional (adiabatic) column, essentially only the middle flat section (pinch zone) is extended while the segments of rapid variation where most entropy is produced are less affected. This means that dissipation for such columns does not approach zero as the number of plates is increased.

The principle of equal thermodynamic distance aims to minimize the total entropy production in the column by distributing it evenly among the plates whatever their number. Nulton et al.[14] optimized a general quasistatic step process, i.e., a process composed of N discrete steps where the system equilibrates fully after each step. The standard description of a distillation column is exactly such a process where it is assumed that gas and liquid come to equilibrium at a particular temperature on each plate. Entropy is produced when the up- and down-moving flows encounter liquid on the next plate at slightly different temperature and composition.

The result of the optimization, for processes not too far from equilibrium, was that the minimum entropy production

$$\Delta S_{\min} = \frac{K^2}{2N} \tag{2}$$

is achieved when the thermodynamic distance D between each pair of plates is kept constant ($D_n = K/N$ for all plates n). K is the total thermodynamic distance from one end of the column to the other. For any other distribution of the total length the dissipation is larger.

The thermodynamic distance is usually measured in the space of all extensive thermodynamic quantities Z_i (energy U, entropy S, volume V, mole numbers N_l, etc.) of the system with the metric[32]

$$M_{ij} = \frac{-\partial^2 S}{\partial Z_i \partial Z_j} \tag{3}$$

evaluated at each equilibrium point in state space. The metric is an equilibrium property defined on the manifold of equilibrium states. The indices i and j represent different extensive thermodynamic quantities. This makes the thermodynamic distance D_n from plate $n-1$ to plate n equal to

$$D_n = \sqrt{\Delta \mathbf{Z}_n \mathbf{M}_n \Delta \mathbf{Z}_n} \tag{4}$$

where $\Delta \mathbf{Z}_n = \mathbf{Z}_n - \mathbf{Z}_{n-1}$ is the difference of the matrix of extensities from plate $n-1$ to plate n and $\mathbf{M}_n$ is the full metric matrix evaluated on plate n. The plate number n is counted from the top down so that plate number 1 is the condenser. The total thermodynamic length of the column is thus

$$K = \sum_{n=1}^{N} D_n \tag{5}$$

Two consequences of this result are the following:[14] (i) The entropy production is equally distributed along the column. (ii) The total entropy production approaches zero as N, the number of plates, goes to infinity; i.e., the separation becomes reversible.

In binary distillation there are 8 extensive quantities involved on each plate, besides the objective function entropy, namely enthalpy, volume, mole number of light component, and mole number of heavy component, each one for both gas and liquid, leading to an 8×8 metric matrix. Fortunately a number of relations allows one to reduce the dimensionality of the problem dramatically. First of all, the two phases are usually considered noninteracting, in which case the matrix $\mathbf{M}$ becomes block-diagonal. Next, constant pressure in the column, energy and mass conservation, and the gas−liquid equilibrium equation reduce the problem to just one free variable which may conveniently be taken to be the temperature. The plate-to-plate distance then becomes simply

$$D_n = \frac{\sqrt{C_{r,n}}}{T_n} \Delta T \tag{6}$$

where $C_{r,n}$ is the plate specific heat capacity involving all the constraints mentioned above, and taking into account the mixing of liquid and gas phases as well as the mixing of thermally different streams (see e.g. refs 18 and 6)

$$C_r = V\left[C_{P,\mathrm{V}} + \frac{T\Gamma_V}{y(1-y)}\left(\frac{\mathrm{d}y}{\mathrm{d}T}\right)^2\right] + L\left[C_{P,\mathrm{L}} + \frac{T\Gamma_\mathrm{L}}{x(1-x)}\left(\frac{\mathrm{d}x}{\mathrm{d}T}\right)^2\right] \tag{7}$$

where $C_{P,\mathrm{V}}$ and $C_{P,\mathrm{L}}$ are the molar heat capacities at constant pressure for the vapor phase and the liquid phase. The Γ's are given by

$$\Gamma_\mathrm{V} = -V\frac{\partial \mu_{2,\mathrm{V}}}{\partial V_1} = -V\frac{\partial \mu_{1,\mathrm{V}}}{\partial V_2}$$

$$\Gamma_\mathrm{L} = -L\frac{\partial \mu_{2,\mathrm{L}}}{\partial L_1} = -L\frac{\partial \mu_{1,\mathrm{L}}}{\partial L_2} \tag{8}$$

where $\mu_{i,\mathrm{V}}$ and $\mu_{i,\mathrm{L}}$ are the chemical potentials of component i in the liquid and vapor phase, respectively. L_i and V_i are the molar flows of component i in the liquid and vapor streams and x and y are the mole fractions of light component in the liquid and vapor, respectively.

The computational procedure then is to integrate eq 6 from the distillate temperature T_D to the reboiler temperature T_B (both of course given by the required product purities) to obtain the total thermodynamic column length K. The distance from one plate to the next must then be fixed at $D = K/N$ for optimal performance by adjusting the plate temperatures appropriately according to eq 6. Obviously such freedom of adjustment does not exist in a conventional adiabatic column. Rather, it is necessary to allow individual heat exchange with each plate to maintain it at the desired temperature. This heat addition/removal is part of the energy balance used above. The result of the whole calculation is either a graph like Figure 3 specifying the temperature of each plate in the column or a graph of the amount of heat added/removed at each plate (Figure 6). It should be emphasized that the total amount of heat used to perform an ETD separation is often only marginally different from that required by a conventional column, but a large part of it is used over a much smaller temperature difference than T_B to T_D leading to a correspondingly smaller entropy production.

3. Equipartition of Force Method Applied to a Diabatic Distillation Column

The EoF optimization method for distillation columns can be summarized as follows (see refs 19 and 28 for further details). The entropy production rate per unit volume θ in a system which transports sensible heat J_q and two components J_i is (see e.g. ref 10)

$$\theta = -J_q\frac{\nabla T}{T^2} - \frac{1}{T}\sum_{i=1}^{2} J_i \nabla \mu_{i,T} \tag{9}$$

Here T is the absolute temperature and the thermal force is $-\nabla T/T^2$. The fluxes are considered positive when transport takes place from the liquid to the vapor. The gradient $\nabla \mu_{i,T}$ is the chemical potential gradient of component i at constant temperature. When the pressure is constant, this is equal to $\nabla \mu_i^c$, the concentration dependent part of the chemical potential gradient. For simplicity the subscript T has been omitted in $\nabla \mu_i^c$. It should be noted that the sensible heat flux J_q can be very different from the total energy flux J'_q which also contains contributions from the enthalpy transported by the mass flux.

The liquid is assumed turbulent. Thus the concentration gradient and the entropy production rate in the liquid phase is assumed to be negligible.[9] The chemical potential gradients in each of the phases are related through the Gibbs−Duhem equation. On this basis we may write the flux equations

$$J_q = -l_{qq}\frac{\nabla T}{T^2} - l_{ql}\frac{y_l \nabla \mu_l}{T} \tag{10}$$

$$J_d = -l_{lq}\frac{\nabla T}{T^2} - l_{ll}\frac{y_l \nabla \mu_l}{T} \tag{11}$$

where l_{ij} are local phenomenological coefficients and $y_l \nabla \mu_l/T$ can be considered the chemical separation force. The coefficients

will be referred to as conductivities. Subscript T has been omitted in $\nabla\mu_l$. The relative diffusion flux J_d has been introduced by the use of the Gibbs−Duhem equation:

$$J_d = \frac{J_l}{y_l} - \frac{J_h}{y_h} \tag{12}$$

The frame of reference for the relative mass flux in eq 12 is the interface between liquid and vapor. We assume that the intensive quantities are constant on the vapor side of the interface region δ so that $\nabla T = \Delta T/\delta$ and $\nabla\mu_l = \Delta\mu_l/\delta$. We neglect the entropy production in the liquid. By introducing this into eq 9, we obtain the entropy production rate of a volume with thickness δ and area A:

$$\Theta = \delta\int^A \theta \, dA = -\frac{\Delta T}{T^2}\int^A J_q \, dA - \frac{y_l\Delta\mu_l}{T}\int^A J_d \, dA \tag{13}$$

The expressions inside the integrals are the fluxes of heat and net mass transport across the area A on a stage in the column. The major simplifications and assumptions behind eq 13 are discussed in refs 27 and 19.

Kjelstrup Ratkje et al.[19] showed that for an ethanol−water distillation the major entropy production at each stage originates from the mass transfer (>98%) rather than from the heat transfer. Thus, according to the principle of equipartition of forces, the thermodynamic driving force for the mass transfer should be made uniform over the column. (In stationary binary distillation only one force can be controlled.)

The irreversible thermodynamic description of distillation of binary mixtures can be combined with the principle of equipartition of forces to obtain optimum operating lines in a McCabe−Thiele diagram. The chemical separation force of eq 11 is $y_l\Delta\mu_l/T$. An EoF operation of the column thus implies that $y_l\Delta\mu_l/T$ is constant over all stages, assuming a constant interface thickness δ.

A McCabe−Thiele diagram for a conventional adiabatic column exhibits a small distance between the operating line and the equilibrium line for the top and bottom parts of the column. Small forces are common because the mixtures in these parts are close to the azeotrope or pure components. In the middle section of the diagram, however, an operating line may be drawn according to

$$y_{l,n+1} = kx_{l,n}\exp\left(\frac{-F}{Rkx_{l,n}}\right) \tag{14}$$

where F is a chosen constant force, k is the constant in Henry's law, n is the stage number, and $x_{l,n}$ and $y_{l,n}$ are the mole fractions of light component in the liquid and vapor phases.[27] If equilibrium trays are assumed, $y_{l,n} = kx_{l,n}$.

If all the mass transfer resistance is in the gas phase, the Gibbs−Duhem equation is strictly applicable, and this is equivalent to equipartitioning of $y_h\Delta\mu_h/T$. It will be shown in Figure 7 that the Gibbs−Duhem equation is only approximately applicable, and it was found that EoF operation based on the heavy component version of eq 14,

$$y_{h,n+1} = kx_{h,n}\exp\left(\frac{-F}{Rkx_{h,n}}\right) \tag{15}$$

gave substantially lower entropy production rates. In the present work the EoF lines are thus based on eq 15. Future works, however, should use a more accurate way to relate the two dependent mass fluxes to each other than by use of the temperature-independent form of the Gibbs−Duhem equation: $\Sigma y_i\Delta\mu_{i,t} = 0$.

TABLE 1: Entropy Produced in the EoF, the ETD, the Conventional Adiabatic, and the Numerically Optimized Columns

column	entropy producn (MJ/(h K))	column	entropy producn (MJ/(h K))
num optimized	1.80	EoF feed adj	1.90
ETD	1.93	conv adiab	2.87
EoF	1.94		

For every choice of F in eq 15, an EoF "line" may be drawn. Care should be taken to get sufficient and well-distributed points on the equilibrium curve. According to the EoF principle these lines represent optimum tradeoffs between entropy production and system size for mass transfer (by diffusion and phase change) between the vapor and liquid streams. As long as the operating line can be modified without (significant) additional entropy production, fluxes, or process size, the EoF lines will also represent optimum tradeoffs between entropy production and system size for the column itself. Columns with small process streams will have minor relative energy costs and should use EoF lines with large driving forces. Larger columns with high energy costs should use EoF lines with smaller driving forces. However, the result eq 15 becomes less valid when large plate-to-plate variations in reflux ratio are required.

4. Simulation of the EoF and ETD Columns

4.1. System Specifications. To compare the EoF and the ETD optimization tools, the separation of an ideal mixture of benzene and toluene was chosen. The mole fraction of both components in the feed was 0.5, and the total amount of feed was 1000 kmol/h liquid at the boiling point. The amount of feed has been chosen in order to reflect a possible industrial column and so that the energy savings attain an industrially relevant magnitude. The results obtained, however, can be directly scaled to any other feed stream.

It was decided to use a column with 17 plates in order to reach 95% purity in both product streams (see ref 35). The condenser on plate 1 is a partial condenser. All plates are considered to be theoretical plates. The reason for the relatively low purity chosen is that the separation to higher purities implies so small driving forces (or thermodynamic steps) that it would limit the size of the forces in the remainder of the column as well. In other words, higher purities would require either a few adiabatic plates in the end sections or a large increase in the total number of plates. Enthalpies, boiling point temperatures, and heat capacities were taken from standard reference handbooks.[7,34]

4.2. Results of the Simulations. Table 1 shows the total entropy production for the EoF column designed according to eq 15, the column with ETD designed according to eq 6, and the numerically found optimal column for the specified purities. The total entropy production was calculated from

$$\Delta S^i = S_{\text{products}} - S_{\text{feed}} + \sum_n \frac{q_n}{T_n} \tag{16}$$

The numerical routine applied to find the best column design was an algorithm making small perturbations on the column in order to find nearby solutions with lower entropy production while maintaining the same separation. The column with the lowest entropy production was chosen, and the perturbation was rerun. Perturbations on the ETD column, the EoF column, and

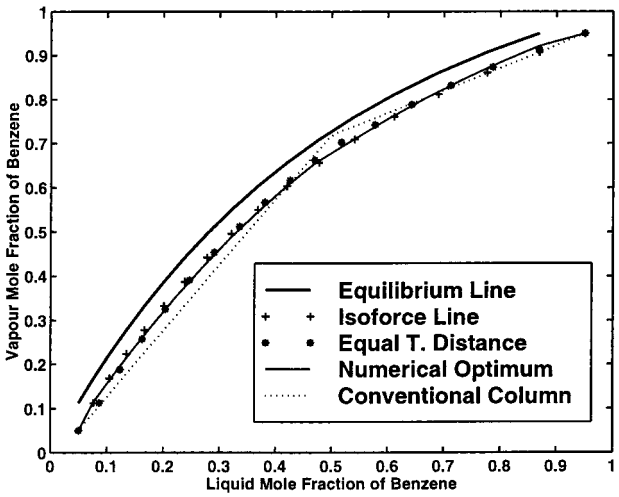

Figure 4. McCabe−Thiele diagram showing the operating lines of the four distillation columns.

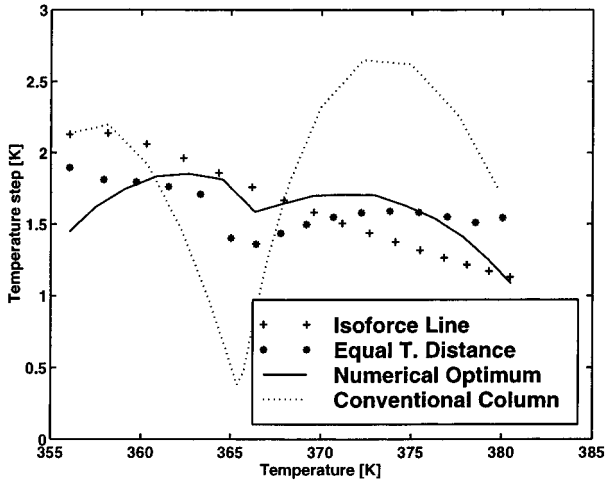

Figure 5. Temperature difference from one plate to the next as a function of plate temperature.

the conventional adiabatic column all ended in the same numerical optimum, thereby strongly indicating that this is indeed the global optimum. The ideal behavior of the mixture separated makes this even more probable.

The ETD and the EoF design principles both clearly predict the numerical optimum far better (i.e. have lower entropy production) than a conventional adiabatic column. A McCabe−Thiele diagram of the four columns presented in Table 1 is shown in Figure 4. Clearly, both the ETD and the EoF operating lines are located close to the numerical optimum, especially when compared with the conventional adiabatic column. Figure 3 similarily shows the temperature profiles of the four columns. As can be seen from both figures, the ETD design appears to predict the numerical optimum slightly better than the EoF design everywhere except at the very bottom part where the EoF operating line is the one closest to the numerical optimum.

The situation is further illuminated in Figure 5 where the temperature steps from plate to plate are plotted as a function of plate temperature. For the separation of two-component mixtures there is a unique relationship between temperature and composition. Thus the relative differences between the columns would be the same if $y_h\Delta\mu_h/T$ had been plotted. The temperature steps between plates are indicative of where dissipation inside the column is located since the mass flows involve mixing of slightly different temperatures and compositions.

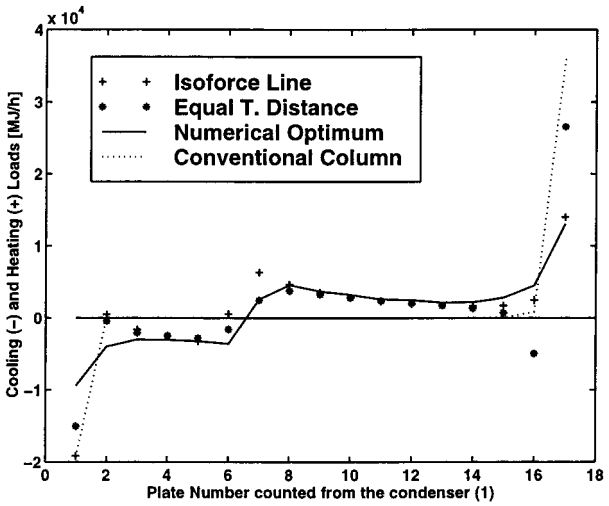

Figure 6. Heating and cooling loads required for the EoF, the ETD, the conventional adiabatic, and the numerically optimized column.

TABLE 2: Total Heating and Cooling Requirements in the EoF, the ETD, the Conventional Adiabatic, the Numerically Optimized, and the EoF Feed-Adjusted Columns[a]

column	tot. heat load (GJ/h)	tot. cooling load (GJ/h)	tot. heat exchanged (GJ/h)	min entropy produced in heat exch (MJ/(h K))
num optimized	43.8	−26.3	70.0	2.59
ETD	46.9	−29.4	76.3	2.82
EoF	44.1	−26.6	70.7	2.62
EoF feed adj	46.5	−29.0	75.5	2.80
conv adiab	36.8	−19.3	56.1	2.08

[a] Included are also the minimum entropy production created in the heat exchangers (with $\Delta T = 5$ K).

As can be seen, the EoF design predicts temperature steps similar to the numerical optimum for temperatures above 378 K while the ETD design is closer for temperatures below 362 K. Figure 5 also shows how both the ETD and the EoF operating lines are able to predict the generally lower temperature steps at high temperatures than at low temperatures. The conventional column, however, behaves completely opposite by creating the largest temperature steps in the bottom section. The EoF operating line does not take the feed into account and therefore fails to predict the reduced temperature steps around the feed point. It is not able to predict the lower steps in the top section but is close to the numerical optimum in the lowermost part of the column. The ETD column predicts quite well the reduction in step size around the feed point, whereas it fails to predict the reduced step sizes at the extremes of the column.

5. Discussion

5.1. Total Entropy Produced. The heating and cooling required for the different columns are shown in Figure 6 and Table 2. For both the ETD and the EoF column designs these loads are adjusted to create the proper thermodynamic length of each step or the magnitude of the driving force. The entropy produced in the heat exchangers required to transfer this heat, or the entropy produced in order to create this heat, being external to the separation process proper, has not been considered in this comparison. In an overall analysis, however, it should of course be included. In Table 2 results are also included for an EoF column adjusted for the feed composition. This column will be further discussed in section 5.2.

TABLE 3: Entropy Production in the Heat Exchangers and Inside the Columns, and the Total Entropy Produced in the Different Columns

column	min entropy produced in heat exch (MJ/(h K))	entropy produced inside column (MJ/(h K))	tot. entropy produced (MJ/(h K))
num optimized	2.59	1.80	4.39
ETD	2.82	1.93	4.75
EoF	2.62	1.94	4.56
EoF feed adj	2.80	1.90	4.70
conv adiab	2.08	2.87	4.95

The entropy produced in the heat transfer to the vapor can be calculated from the first term of eq 13 where the integral simply is the amount of heat transferred. As a best case we assume that the driving forces for heat exchange are equal on all the plates. The force chosen $\Delta T/T^2 = 5\ \mathrm{K}/(370\ \mathrm{K})^2$. $T = 370$ K represents the approximate average temperature of the column. The small temperature difference (5 K) chosen for the heat exchangers is in the lower range of what is economically possible, but since the boiling points of the top and bottom products are so close, the gain of the optimization would almost disappear if large temperature differences were used in the heat exchanges. The entropy produced in the heat exchanges is then strictly proportional to the heat exchanged and can be calculated from the first term of eq 13; these data are summarized in Table 2.

As the entropy production rates in the heat exchangers are not part of the objective function in any of the optimized columns, it was almost obvious that these would increase compared with the conventional adiabatic column. As can be seen from Table 3, however, there is still a net reduction in the total entropy production when these additional losses are included. The size of these reductions is limited because the boiling points of the two products are fairly close. The effect of using different temperature utilities must then obviously become small. For larger differences in boiling point temperatures between the products, the gains will necessarily be higher. The main aim of this work is to evaluate the generic results of the two methods on a simple example.

It should also be pointed out that the difference between the ETD column and the two other heat integrated columns in Tables 2 and 3 is solely due to the large step required by ETD on the bottom plate; see Figure 5. This step size could not be obtained without inserting a local cooler on the plate above the bottom plate, thereby forcing the reboiler load to increase by the same amount. The reason for this oddity is that a total of 17 plates is barely enough to permit ETD operation. With a few additional plates this artifact would disappear.

5.1.1. A Broad Optimum. The entropy amounts produced inside the ETD, the EoF, and the numerically optimized columns are all quite similar as is shown in Table 1. At the same time, however, the three columns have distinctly different temperature and composition profiles; see e.g. Figure 3. Thus the optimum column design appears to be a fairly flat optimum where considerable variations in the profile create only small variations in the overall entropy production rate. Whether this situation is the same for the separation of nonideal and/or multicomponent mixtures remains to be seen.

The results presented in Figures 3−6 for the separation of an ideal mixture are not sufficient for a complete evaluation of the EoF and ETD design principles. However, some of the accomplishments and future challenges can be identified by comparing the results with the knowledge of how the two column design tools were arrived at. Thus, below, the differences between the two theoretically derived columns and the numerically optimized one are summarized and related to assumptions or prerequisites in the theories.

5.2. Comparison of EoF and Numerically Optimized Operation. The agreement between the EoF column and the numerical optimum in Figures 3−6 appears to be quite good except for the large reflux ratios predicted in the top section (see Figure 6) and the lack of a feed point correction. This relative success is further supported by the implemented improvement of a ternary distillation column at Norsk Hydro Rafnes in May 1998, where the feed streams were modified according to the EoF principle (see refs 22, 36).

5.2.1. Mass Flows Created by the Intermediate Heat Exchangers. There are several factors which contribute to making the EoF operating lines only approximately optimal. First, the mass flows created by the intermediate heat exchangers are not accounted for in the derivation of the EoF operating lines. The EoF line itself merely optimizes the diffusion, evaporation, and condensation processes between the vapor and liquid phases while the bulk mass transfer created by the intermediate heat exchangers are not taken into account. Thus, when the bulk mass transfer becomes dominant (e.g. at large reflux ratios) the EoF operating lines become less relevant.

A consequence of the ETD column design is that entropy production is distributed uniformly among the plates. That is not the case for the EoF design even though variations are small. The lack of handling of the mass flows due to the intermediate heat exchangers is the primary source of this discrepancy. Since the additional mass flow builds up in the stripping (lower) section of the distillation column and diminishes again in the rectifying (upper) section, we can see this shift of temperature and composition as an upward bulge of the EoF line in Figure 3.

5.2.2. Gibbs−Duhem Equation. An important factor in the derivation of the EoF schedule is the applicability of the Gibbs−Duhem equation. This equation relates the chemical potentials of different components in a single phase and is hence applicable in the way it is used here only if all the mass transfer resistance is associated with the vapor phase. Until now EoF operating lines have been designed according to eq 14 with the mole fractions representing the light component. According to the Gibbs−Duhem equation, which was applied in the derivation of eq 14, these lines should be equivalent to operating lines based on the heavy component. Exchanging the mole fractions of the light component with those of the heavy component (eq 15), however, reduced the entropy production in the column by more than 10%; in this work only the heavy component based lines are presented. Figure 7 shows the deviations from the Gibbs−Duhem equation in the column in that the light and heavy component forces should be the same.

As can be seen in Figure 7, the light component force $y_l\Delta\mu_l$ is systematically larger (in absolute value) than the heavy component force $y_h\Delta\mu_h$. The difference is smallest in the middle and larger in the end sections thereby illustrating why a design with driving forces based on eq 14 specifies larger forces in the end sections (and performs worse) than a column based on eq 15. As mentioned above, the systematic mismatch in Figure 7 may be due to the location of some mass transfer resistance in the liquid phase as well as in the vapor phase. But, as will be further supported by Figure 9 below for a larger column, the deviation from a $y_l\Delta\mu_l/y_h\Delta\mu_h$ ratio of 1 in Figure 7 may also be due to the implicit assumption

$$\Delta\mu_l = \mu_{l,T_n,n} - \mu_{l,T_{n+1},n+1} = \mu_{l,n} - \mu_{l,n+1} \qquad (17)$$

which was not realized in previous works.[19, 27]

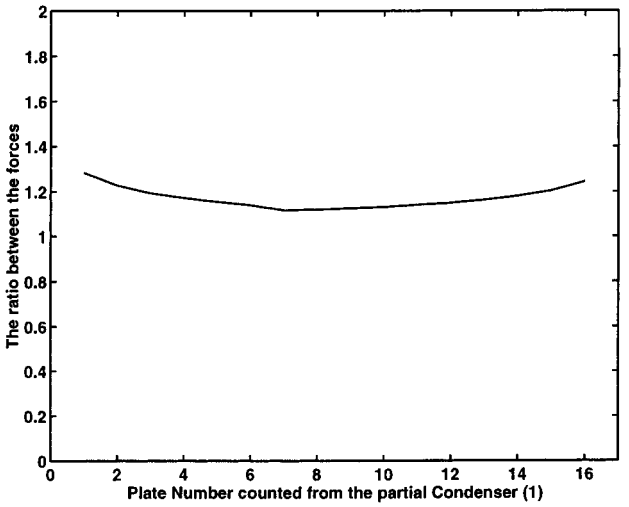

Figure 7. Ratio of $y_l\Delta\mu_l$ over $-y_h\Delta\mu_h$ for the different plates in the distillation column. The Gibbs−Duhem equation is strictly applicable only when the ratio is equal to unity.

If we consider that

$$\left[\frac{\partial}{\partial T}\left(\frac{\partial G}{\partial n_1}\right)_{T,P,n_j}\right] = \left(\frac{\partial G_1}{\partial n_1}\right)_{P,n_j} = -S_1 \tag{18}$$

where n_j is the number of moles of component j, we find that

$$\mu_{l,T_2} - \mu_{l,T_1} = -S_l(T_2 - T_1) \tag{19}$$

which may be part of the reason for the lack of agreement between eqs 14 and 15. This may also contribute to explaining why the EoF temperature steps in the 40 plate column shown in Figure 9 below have a greater spread than the numerically optimized steps. It may thus be recommended for future work to apply the full Gibbs−Duhem equation (see e.g. ref. 26)

$$\left(\frac{\partial G}{\partial P}\right)_{T,x} \mathrm{d}P + \left(\frac{\partial G}{\partial T}\right)_{P,x} \mathrm{d}T - \Sigma x_i \,\mathrm{d}\mu_i = 0 \tag{20}$$

which at constant pressure reduces to

$$-\bar{S}\,\mathrm{d}T - \Sigma x_i \,\mathrm{d}\mu_i = 0 \tag{21}$$

At constant pressure we may approximate the difference in chemical potential for component l from vapor stream n to $n+1$ as

$$\mu_{l,T_n,n} - \mu_{l,T_{n+1},n+1} = \mu^c_{l,n} - \mu^c_{l,n+1} - S_l(T_n - T_{n+1}) \tag{22}$$

which according to eq 21 is equivalent to

$$-(\mu^c_{h,n} - \mu^c_{h,n+1} - S_h(T_{n+1} - T_n)) \tag{23}$$

In future works either of these relations (eq 22 or 23) should be applied rather than the simplified Gibbs−Duhem equation. Then the driving forces in the EoF column will become more uniform and it will probably contribute to making the EoF line in Figure 9 more similar to the numerical optimum, especially since the new term is proportional to ΔT.

5.2.3. Mixing of Liquid Phases. As for instance Taprap and Ishida[29] have shown, the exergy losses due to mixing of the liquid phases from neighboring plates may contribute significantly to the total exergy losses in distillation columns. These losses were not explicitly taken into account when the EoF operating lines were derived. However, the optimal distribution of exergy losses from the mixing process is closely correlated with the optimal distribution of exergy losses from the mass transfer process. This may contribute to explaining why an optimization of the diffusion, evaporation, and condensation processes only (the EoF lines) still gives results close to the numerical optimum for the overall internal column process.

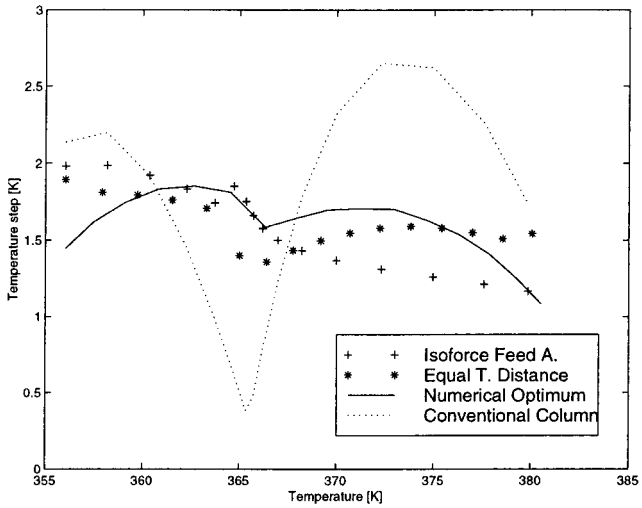

Figure 8. Temperature difference from one plate to the next as a function of plate temperature for the feed adjusted EoF column compared to the numerical optimum, the ETD, and the conventional columns.

5.2.4. Feed Point Correction. The effects of the missing feed point adaption may probably be reduced by taking the feed composition as a plate composition and then equipartitioning the forces in the upper and lower column sections separately rather than for the whole column simultanously. The forces above and below the feed point will then necessarily be somewhat different. Since the column section above the feed point (the rectifying section) requires continuous cooling, energy dissipation in this section is presumed to be worse than energy dissipation in the stripping section below the feed point. We therefore performed a numerical simulation where the force was slightly reduced above the feed point and slightly increased below the feed point until the feed composition matched the feed plate composition. As can be seen in Figure 8, the temperature steps for the EoF column around the feed point in this way came significantly closer to the numerical optimum.

5.2.5. Total Entropy Production. A fundamental weakness of both the EoF and the ETD design principles with respect to practical application is the decision not to include the entropy production in the intermediate heat exchangers in the objective function. This decision was made deliberately to focus on the separation process proper as distinct from the peripheral equipment. Nonetheless, as Table 2 shows, this did imply an increasing amount of heat exchanged for the EoF and the ETD columns compared to the conventional adiabatic column. In general the total heat exchanged must increase in a column with distributed heat exchange compared to the adiabatic case when the same product shall be produced on the same number of plates since reflux will be reduced in some parts of the column. To compensate for that reduction and concomitant lower separation contribution, reflux must increase in other parts.

For columns with larger temperature spans between the top and bottom products the entropy production in the heat exchangers will become proportionally smaller. For multicomponent separations there will also often be more parameters available for driving force optimization than just the exchange of heat, like for example feed stream distribution and side products.

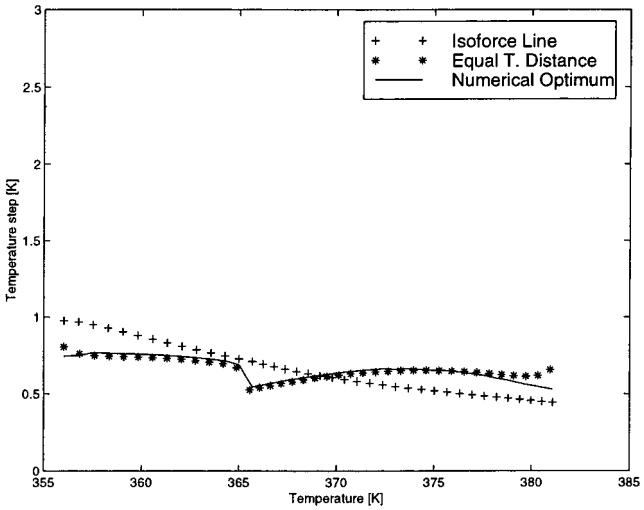

Figure 9. Temperature difference from one plate to the next as a function of plate temperature for a column with 40 plates.

5.3. Comparison of the ETD and Optimal Operating Lines. The agreement between the ETD column and the numerical optimum in Figures 3−6 is quite good except for the large step sizes and reflux ratios predicted by ETD in the very end sections. The optimal situation around the feed point is predicted well by the ETD column as shown in Figures 5 and 6.

Before a further discussion is carried out, it will be beneficial to look at the results in Figure 9 of a 40 plate ETD column compared to the numerical optimum and the EoF prescription.

As can be seen, the ETD design predicts almost completely the numerical optimum except for some small deviations in the end sections. Thus it can be concluded that the ETD theory predicts the numerically optimal column almost completely for large plate numbers but fails somewhat (mainly in the end sections) for smaller plate numbers and larger step sizes.

The difference between the ETD column and the two other heat integrated columns in Table 2 is solely due to the large step required by ETD on the bottom plate for this small system; see Figure 5. This step size could not be obtained without the counterintuitive introduction of a local cooler on the plate above the bottom plate, thereby forcing the reboiler load to increase by the same amount. The total heat exchanged increased by approximately 6 GJ/h due to this step only. The reason for this unusual construction is that the 17 active plates intially chosen for the present comparison is just not long enough to secure a proper ETD profile. Increasing the number of plates will alleviate the need for an intermediate cooler and associated increased boiler load. The results for the large column in Figure 9 shows this clearly.

The ETD design prescription is identical to the leading term in an asymptotic expansion of the entropy production for large number of plates, N. The term with $N = \infty$ corresponds to reversible operation, while the term of order N^{-1} is predicted by ETD.[15] Numerical optimization is of course not restricted to powers of N^{-1} but provides the exact optimum. Thus it is quite clear that ETD will show discrepancies with the fully numerical optimization for small N while being identical to it for large N (see also ref 23 for a more complete numerical comparison).

5.4. Physical vs Economic Optimum. It is important to keep in mind that the EoF and the ETD designs are only attempts to find a physical optimum between entropy production and column size. This is not equivalent to the economic optimum,[33] although there is a strong correlation between the two. The EoF lines and the ETD lines rather provide the engineer with a good initial *estimate* for cost-optimal designs and also provide the engineer with a *reference* to the most energy efficient design.[25]

5.5. Benchmark for Distillation Columns. Agrawal and Woodward[3] have suggested using reversible distillation as a "bench mark" (or "minimum thermodynamic condition"[8]) for measuring the efficiency of a real column. Since such reversible columns are not practically attainable, they are not really fit for benchmarking. We rather propose that the ETD or EoF column be much better bench marks for real columns since they do include operational irreversibilties.

5.6. Toward Multicomponent Distillation. Equipartition of forces can be extended to multicomponent systems in several ways. If enough degrees of freedom are available, the driving force $\Delta\mu_k/T$ for each component may be equipartitioned. This approach was used by Sauar[22] for improving a distillation column separating HCl from vinyl chloride monomer (VCM) and ethylene dichloride (EDC) at Norsk Hydro Rafnes in Telemark, Norway. Another possibility is to apply eq 15 to optimize the separation between two key components.

The ETD theory outlined in section 2 is not restricted to two-component systems. More components will simply make the metric matrix **M** defined in eq 3 larger by including the additional mole numbers. The following mathematical reduction of the resulting larger system of equations will follow the same lines as in section 2, but one will not necessarily arrive at a final expression in terms of a single parameter, e.g. the temperature, since ternary and higher mixtures have more degrees of freedom.

6. Conclusion

The equal thermodynamic distance (ETD) and equipartition of forces (EoF) design principles have been applied to binary distillation and compared with a numerically determined optimum. The entropy production inside the ETD column, the EoF column, and the numerically optimized column was found to be 32.8%, 32.6%, and 37.3% less than in the conventional adiabatic column, respectively. The difference between the EoF column and the numerically optimized column occurs mainly in the end sections where the EoF operating line requires driving forces that are hardly available because of the mass balance. The mismatch is mainly due to (i) failure to take bulk flows into account, (ii) mass balance restrictions on the driving force in the upper section, and (iii) uncertainty in the application of the Gibbs−Duhem equation. The ETD column differs from the numerical optimum much in the same manner as the EoF column, by requiring step sizes in the end sections which the mass balance cannot allow or only allows at high entropy costs. For larger plate numbers, however, the ETD column is almost in complete agreement with the numerical optimum.

Acknowledgment. This work is supported by the Danish Natural Science Research Council, Contract 28808. G.S. and E.S. wish to thank the Ørsted Laboratory for its hospitality.

List of Symbols

A = surface (transfer) area
C = heat capacity
D = thermodynamic distance
Ex = exergy
F = constant (force)
G = Gibbs free energy
J = flux
K = thermodynamic length
L = liquid rate

M = Weinhold metric
N = total number of plates
P = pressure
R = gas constant
S = entropy
T = temperature
U = internal energy
V = vapor rate
W = work
x = mole fraction of light component in liquid phase
y = mole fraction of light component in vapor phase
Z = extensive thermodynamic properties

Greek Letters

δ = thickness of gas interface
Δ = difference
Γ = defined in eq 8
∇ = gradient
μ = chemical potential
θ = local entropy production rate per unit volume
Θ = total entropy production rate

Subscripts

d = diffusion
h = heavy componet
i, j = indexes for external properties
i, 1, 2 = component indexes
k = Henry's constant
l = light component
L = liquid stream
n = plate number
P = pressure
q = sensible heat
r = constant pressure saturation heat capacity index
R = real
V = vapor stream
0 = reference state (the surroundings)

Superscripts

irr = irreversible
$\cdot$ = rate
c = concentration dependent

References and Notes

(1) Aguirre, P.; Espinosa, J.; Tarifa, E.; Scenna, N. Optimal thermodynamic approximation to reversible distillation by means of interheaters and intercoolers. *Ind. Eng. Chem. Res.* **1997**, *36*, 4882−4893.

(2) Agrawal, R.; Fidkowski, Z. T. On the use of intermediate reboilers in the rectifying section and condensers in the stripping section of a distillation column. *Ind. Eng. Chem. Res.* **1996**, *35*, 2801−2807.

(3) Agrawal, R.; Woodward, D. W. Cryogenic nitrogen generators: An exergy analysis. *Gas Sep. Purif.* **1991**, *5*, 139.

(4) Andresen, B. *Finite-Time Thermodynamics*; Physics Laboratory II, University of Copenhagen: Copenhagen, 1983.

(5) Andresen, B.; Gordon, J. M. Constant thermodynamic speed for minimizing entropy production in thermodynamic processes and simulated annealing. *Phys. Rev. E* **1994**, *50*, 4346−4351.

(6) Andresen, B.; Salamon, P. Optimal distillation using thermodynamic geometry. In *Thermodynamics of Energy Conversion and Transport*; Sieniutycz, S., De Vos, A., Eds.; Springer: Berlin, 2000.

(7) *Handbook of Chemistry and Physics*; Chemical Rubber Co.: Boca Raton, FL, 1997.

(8) Dhole, V. R.; Linnhoff, B. Distillation column targets. *Comput. Chem. Eng.* **1993**, *17*, 549−560.

(9) Duineveld, P. C. Bouncing and coalesence of two bubbles in water. Doctoral Thesis 169, University of Twente, 1994.

(10) Førland, K. S.; Førland, T.; Kjelstrup Ratkje, S. *Irreversible Thermodynamics, Theory and Applications*; Wiley: Chichester, U.K., 1988.

(11) Fonyo, Z. Thermodynamic analysis of rectification: 1. Reversible model of rectification. *Int. Chem. Eng.* **1974**, *14*, 18−27.

(12) Kaiser, V.; Gourlia, J. P. The ideal column concept: Applying exergy to distillation. *Chem. Eng.* **1985** (Aug 19), 45−53.

(13) King, C. J. *Separation Processes*; McGraw-Hill: New York, 1971.

(14) Nulton, J.; Salamon, P.; Andresen, B.; Qi, A. Quasistatic processes as step equilibrations. *J. Chem. Phys.* **1985**, *83*, 334−338.

(15) Nulton, J.; Salamon, P. Asymptotic behavior of claimed optimal thermodynamic paths. Manuscript in preparation.

(16) Rivero, R. Exergy simulation of a distillation tower: Diabatic stripping column. In *Efficiency, Costs, Optimization, Simulation and Environmental Impact of Energy Systems*; Gögüs, Y. A., Öztürk, A., Tsatsaronis, G., Eds.; Istanbul, 1995; Vol. 1, pp 163−167 (ISBN 975-7475-06-8).

(17) Rivero, R. Exergy simulation of a distillation tower: Diabatic rectification column. In *2nd Law Analysis of Energy Systems: Towards the 21st Century*; Sciubba, E., Moran, M. J., Eds.; ASME, Rome, 1995; pp 465−476.

(18) Rowlinson, J. S. *Liquids and Liquid Mixtures*; Plenum Press: New York, 1969.

(19) Kjelstrup Ratkje, S. K.; Sauar, E.; Kristiansen, E. M.; Lien, K.; Hafskjold, B. Analysis of entropy production rates for design of distillation columns. *Ind. Eng. Chem. Res.* **1995**, *34*, 3001−3007.

(20) Salamon, P.; Berry, S. Thermodynamic length and dissipated availability. *Phys. Rev. Lett.* **1983**, *51*, 1127.

(21) Salamon, P.; Nulton, J. The geometry of separation procesees: A horse-carrot theorem for steady flow systems. *Europhys. Lett.* **1998**, *42*, 571−576.

(22) Sauar, E. Process Design by Optimum Entropy Production. M.Sc. Thesis, Department of Physical Chemistry, NTNU, 1994.

(23) Schaller, M.; Hoffmann, K. H.; Siragusa, G.; Salamon, P.; Andresen, B. Numerically optimized performance of diabatic distillation columns. Submitted to *Comp. in Chem. Eng.*

(24) Sauar, E.; Rivero, R.; Ratkje, S. K.; Lien, K. M. Diabatic column optimization compared to isoforce columns. *Energy Conv. Mgmt.* **1997**, *38*, 1777−1783.

(25) Sauar, E.; Kjelstrup, S. K.; Lien, K. M. Rebuttal to Comments on 'Equipartition of forces: A new principle for process design and optimization'. *Ind. Eng. Chem. Res.* **1997**, *36*, 5045−5046.

(26) Smith, J. M.; Van Ness, H. C. *Introduction to Chemical Engineering Thermodynamics*, 4th ed.; McGraw-Hill: New York, 1987.

(27) Sauar, E.; Kjelstrup Ratkje, S. K.; Lien, M. Process optimization by equipartition of forces. Applications to distillation columns. In *Efficiency, Costs, Optimization, Simulation and Environmental Impact of Energy Systems*; Gögüs, Y. A., Öztürk, A., Tsatsaronis, G., Eds.; Istanbul, 1995; Vol. 2, pp 413−418 (ISBN 975-7475-06-8).

(28) Sauar, E.; Kjelstrup Ratkje, S.; Lien, K. M. Equipartition of forces. A new principle for process design and operation. *Ind. Eng. Chem. Res.* **1996**, *35*, 4147−4153.

(29) Taprap, R.; Ishida, M. Graphic exergy analysis of processes in distillation column by energy utilization diagrams. *AIChE J.* **1996**, *42*, 1633−1641.

(30) Terranova, B. E.; Westerberg, A. W. Temperature−heat diagrams for complex columns. 1. Intercooled/interheated distillation columns. *Ind. Eng. Chem. Res.* **1989**, *28*, 1374−1379.

(31) Tolman, R. C.; Fine, P. C. On the irreversible production of entropy. *Rev. Mod. Phys.* **1948**, *20*, 51−77.

(32) Weinhold, F. Metric geometry of equilibrium thermodynamics. *J. Chem. Phys.* **1975**, *63*, 2479.

(33) Xu, J. Comments on 'Equipartition of forces: A new principle for process design and optimization'. *Ind. Eng. Chem. Res.* **1997**, *36*, 5040−5044.

(34) Yaws, C. L. *Thermodynamic and Physical Property Data*; Gulf Publ. Co.: Houston, TX, 1992.

(35) The driving forces in the end sections required by the ETD and the EoF column designs cannot be realized for plate numbers close to N_{min}, where a conventional column is the only possibility. A total of 17 plates was chosen because it is around the minimum number of plates which is necessary in order to use ETD and the EoF operation in the complete column and not only in the middle of the rectifying and stripping sections.

(36) In brief, a hot vapor stream rich in the *light* component is now fed further down into a column separating HCl from vinyl chloride monomer (VCM) and ethylene dichloride (EDC) at Norsk Hydro Rafnes. The chemical potential of the light component in the feed stream matched better with the chemical potential in the bottom of the column (although the concentration match was better further up). The heat of the vapor stream could then be used to heat the down coming liquid gradually at each plate rather than as a "heat shock" on the original feed plate.